LBL-26980 c.2
Preprint

Lawrence Berkeley Laboratory
UNIVERSITY OF CALIFORNIA

APPLIED SCIENCE DIVISION

Submitted to Environmental Science and Technology

Modeling and Field Evidence of Pressure-Driven Entry of Soil Gas into a House through Permeable Below-Grade Walls

K. Garbesi and R.G. Sextro

March 1989

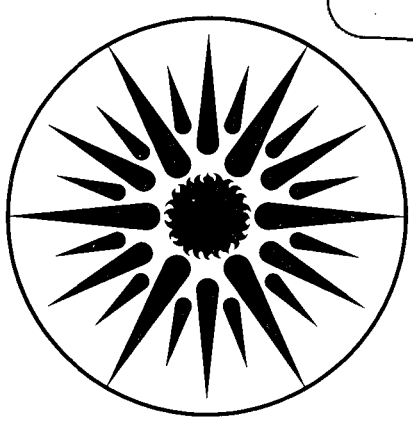

APPLIED SCIENCE DIVISION

Prepared for the U.S. Department of Energy under Contract Number DE-AC03-76SF00098.

DISCLAIMER

LBL-26980

Submitted to *Environmental Science and Technology*

MODELING AND FIELD EVIDENCE OF PRESSURE-DRIVEN ENTRY OF SOIL GAS INTO A HOUSE THROUGH PERMEABLE BELOW-GRADE WALLS

K. Garbesi and R.G. Sextro
Indoor Environment Program
Applied Science Division
Lawrence Berkeley Laboratory
1 Cyclotron Road
Berkeley, CA 94720

March 1989

This work was supported by the Occidental Chemical Corporation under Agreement No. BG 8602A and by the Assistant Secretary for Conservation and Renewable Energy, Office of Building and Community Systems, Building Systems Division of the U.S. Department of Energy under Contract No. DE-AC03-76SF00098.

Abstract

Modeling and field evidence are presented which indicate that soil gas can enter houses with basements at significant rates through permeable below-grade walls. Entry via this previously neglected pathway could result in elevated indoor concentrations of radon and other pollutants. Using artificial depressurization of the basement (-25 to -30 Pa), field measurements were made of pressure-coupling between a basement and the surrounding soil and of soil-gas entry into the house . A two-dimensional, steady-state finite element model of fluid flow through porous media was used to simulate the experimental conditions, assuming air flow occurs through permeable substructure walls. The model predicts a soil-gas entry rate of 2.5 m^3hr^{-1}. The best estimate of soil-gas entry, based on field tracer-gas studies, was 4 m^3hr^{-1}, with a range of 1.5-12 m^3hr^{-1}. The soil was modeled with and without a low-permeability layer just above basement floor level. The layered-soil model explains high pressure-coupling observed at 3-m depth out to 14 m west of the house.

Introduction

Soil gas is an important source of indoor air pollution. Research on sources of human exposure to radon indicates that soil is the primary source of indoor radon in single-family houses in the United States (1). Pressure-driven flow is a principal means by which soil gas enters houses; it is expected to be the predominate source of radon in houses with elevated concentrations (2,3,4). Recent studies indicate that entry of volatile organic contaminants via the soil-gas pathway could pose a public heath risk in residences located near landfills, even those designated to accept only non-hazardous waste (5,6).

Pressure-driven flow of soil gas into houses results from the depressurization of the substructure of the house with respect to the surrounding soil. There are three principal causes of basement depressurization: thermal differences between indoors and outdoors, wind-loading on the building superstructure, and/or imbalanced building ventilation (2,4). Field measurements have shown that under normal operating conditions of houses during the winter, the temperature effect alone can result in consistent substucture underpressures between 2 and 6 Pa (7,8). Other factors being equal, pressure-driven entry is likely to be most important in houses with basements because they provide a large interface with the soil. Soil-gas entry due to basement depressurization has been experimentally demonstrated by Turk *et al.* (9) and Nazaroff *et al.* (10). Significant pressure-driven entry of radon from soil has also been reported for houses with crawl spaces (11). Entry pathways have been assumed to be penetrations, gaps, or cracks in the building substructure (10,12,13,14,15).

Pollutant transport through permeable substructure walls has been considered in the context on radon entry into residential buildings, but, to our knowledge, has not yet been incorporated in exposure-assessment modeling. Marynowski (16) and Harris *et al.* (17) conducted laboratory studies of air flow through cement-block walls. Their results indicate that significant air flow can occur through this type of wall, even at low pressure-differentials.

Marynowski measured an air flow rate of 1.3 x 10^{-5} ms^{-1} (13 cm^3s^{-1} per m^2 of wall area) for uncoated, hollow cement-block wall at an applied pressure difference across the wall of 10 Pa, and measured a flow rate of 1.3 x 10^{-6} ms^{-1} (1.3 cm^3s^{-1} per m^2) for hollow cement-block wall sealed with a mortar coating. Harris *et al.* measured a flow rate of 1.6 x 10^{-4} ms^{-1} (160 cm^3s^{-1} per m^2) for uncoated, hollow wall at a one Pa pressure differential under similar experimental conditions. The difference was probably due to different physical characteristics of the cement blocks and/or mortar material in the different experiments.

Numerical (computer) and analytical (closed form) models have been developed to predict pressure-coupling between a basement and the surrounding soil and to predict soil-gas and radon entry (10,13,14,15). These models restrict the soil-gas entry pathway to a gap at the basement wall-floor interface. This treatment arises because, in many cases, a basement is constructed by pouring a cement-slab floor inside a previously constructed cement footer or frame. Upon drying, slab shrinkage produces a peripheral gap. The peripheral-gap geometry has also been used to represent entry through a perimeter drain-tile system connected to a basement sump through an untrapped pipe (12). Most of models assume unsaturated, homogeneous, isotropic soil (10,13,15). The Loureiro (14) model allows different soil properties to be assigned to regions of soil adjacent to the basement wall and floor (areas frequently modified during house construction). Nazaroff *et al.* (10) used an analytical model based on an electrical analog to simulate pressure coupling induced by artificial basement depressurization at a field-study house. The model underpredicted the measured values by more than a factor of ten. The authors hypothesized that their predictions might be low due to layering of dissimilar soils, a factor for which their model did not account.

In this paper, we present field evidence and modeling results of soil-gas entry into a house with a basement via permeable substructure walls. The permeable wall approach was first considered because basement construction of the study house was not of the type likely to produce a gap at the wall-floor interface, and no evidence of such a gap was observed. The slab and footer of the study house were poured as one piece. The concrete block wall was

then built on top of the footer. Water damage on a large section of the interior walls indicated that gas flow across the walls could be possible.

A two-dimensional, steady-state finite element model of fluid flow through porous media is used to simulate the conditions of the field experiments. The soil is modeled both with and without a low-permeability soil layer just above the depth of the basement floor (as indicated by field observations). The results of the modeling are compared with field measurements of the pressure-coupling between the basement of the house and the surrounding soil and with data on soil-gas entry into the basement. The difference in potential for soil-gas entry through permeable walls versus that through a perimeter gap are examined by comparing the results of the present model with predictions from the perimeter gap models of Loureiro (14), Mowris (13), and Mowris and Fisk (15).

Field Measurements

The study site was a unoccupied, single-family residence located in Central California. The site is level to the north and west, but slopes abruptly down from the house on the south and south east (Figure 1). The house is a three bedroom, one-story structure built over a basement and garage, which terminate at a depth of 2.5 m below grade. The basement walls were constructed of hollow cement blocks. The walls were then backfilled with cement and coated with an asphalt sealant on the exterior. The interior walls and floor of the basement were painted, but otherwise bare. The areas of the first floor and basement are 183 and 103 m^2, respectively. A complete description of the study site and field measurements may be found in Hodgson *et al.* (6). The results are briefly summarized here.

Pressure coupling between the basement and the surrounding soil was measured using the technique of Nazaroff *et al.* (10). With the basement of the study house depressurized by a blower door (large fan) to 25 Pa below atmosphere, pressures were measured in soil probes distributed around the house at depths ranging between 1.0 and 3.2 m. The majority of the measurements were made on the west side of the house because of easier access to the soil

surface. Figure 1 indicates the measured pressure-coupling (in percent of basement underpressure) at the probe locations. Pressure coupling was fairly evenly distributed about the house. Coupling on the west side of the house was generally observed to be between 30 and 37 percent for probes 0.5 m from the basement wall and 1.5-m deep. Coupling decreased smoothly with increasing distance out to 5 m from the house. At distances greater than 5 m, coupling showed a sudden increase. This was probably due to irregularity in the large-scale structure of the soil, with increased coupling reflecting a zone of increased permeability between the basement and the far field. Because the simple soil geometries modeled in this study will not predict such variation, we make quantitative comparisons between the model and the data only out to 5 m from the house. The comparison is made for probes of 1.5-m depth since the greater number of measurements at this depth provided a better characterization of the soil pressures.

Air-permeability measurements of the soil were also made at all of the probes. Based on resistance during probe insertion, there appeared to be a dense, hard layer approximately one half meter thick lying between a 2- and 3-m depth, depending on probe location. Probes were generally terminated either above or below this layer because within the layer excessive resistance to air flow made permeability measurements impossible with the available equipment. Therefore, mean permeabilities calculated from the in-situ measurements apply to the bulk soil, but not to the low-permeability layer. The mean permeability of the bulk soil (above and below the low-permeability layer) was 3×10^{-12} m^2 with a range of 0.3 to 20×10^{-12} m^2. Permeability of the soil in the dense layer was estimated by an indirect method. Soil samples were collected by bucket auger and analyzed for particle size distribution to determine the USDA soil type. Samples taken from the layer were of the silt-loam type, associated with an air permeability range of 10^{-14} to 10^{-13} m^2 (4). Samples taken from the bulk soil were of the sandy-loam and loamy-sand types, which have a permeability range of 10^{-13} to 10^{-11} m^2.

Soil-gas entry into the house was measured using a tracer-gas technique similar to that of

Nazaroff (10). Sulfurhexafluoride (SF_6) was injected into the soil in numerous probes on the north and west sides of the house. One month later, SF_6 was detected in the soil gas at all probes. Dichlorofluoromethane (Freon-12) was also distributed throughout the soil, apparently having migrated onto the site from the adjacent municipal landfill. Both compounds were detected by on-site gas chromatography (GC).

After purging the basement with fresh, surface air, the basement was sealed and depressurized by blower door. Soil-gas entry rates were determined by monitoring basement concentrations of SF_6 and Freon-12 while incrementally increasing basement depressurization. Soil-gas entry into the house was estimated from the experimental data using a simple mass-balance model. Two factors combine to introduce considerable uncertainty into this estimate. First, the soil-gas tracers were inhomogeneously distributed in the soil resulting in uncertainties in the average concentration in the soil on different sides of the house. Second, the actual leakage geometry of the basement was not known. The technique was therefore only able to give an approximate estimate of entry rate. At a basement depressurization of 30 Pa, the best estimate of the rate of soil-gas entry into the basement was 4 m^3hr^{-1}, with a possible range of 1.5 to 12 m^3hr^{-1}.

Model Description

Flow of soil gas through unsaturated soil (at driving-force pressures induced in the field experiment or under normal house operating conditions) obeys Darcy's Law of flow through porous media (4,18). Darcy's Law for the pressure-driven flow of soil gas is written:

$$v = - k/\mu \nabla P , \qquad (1)$$

where v is the volumetric fluid flux, k is the permeability of the soil to air, μ is the viscosity of soil gas (taken as the viscosity of air), and P is the disturbance pressure (total pressure minus atmospheric pressure).

To model the soil-gas response to basement depressurization, we used a standard two-dimensional, steady-state finite element model of fluid flow through porous media. The model

was run on an IBM PC AT. Such models are in common use to solve groundwater flow problems (19). These models apply Darcy's Law across each element under the constraints imposed by the user-defined boundary conditions. (The rapid attainment of steady-state soil pressures observed in the field after imposed changes in basement pressure indicated that a steady-state model was applicable.)

The field site was modeled by taking an east-west cross-section at the mid-point of the basement. All model boundaries were designated as flux boundaries. The soil surface and the interior of the basement wall and floor were designated as constant pressure boundaries. The modeled region was terminated 42 m to the west of the house and 8.5 m below the soil surface to ensure that pressure predictions within the probe-field region would be insensitive to boundary effects. The basement wall and floor were incorporated as elements in the flow-net and assigned a thickness of 0.25 m. To minimize the computational effort, variable sized elements were used. Finer mesh was used to define the basement walls and floor and the probe field region. Coarse mesh was used in outlying areas, thereby limiting the total number of nodes to 196.

To mimic conditions of the field experiment, all cases of the model were run using soil surface and basement interior pressures of zero and -30 Pa, respectively. Since the percentage of the basement pressure seen by the soil is unchanged by the choice of basement pressure, the modeling predictions, expressed as fractional depressurizations, could be compared with pressure-field measurements which where made at -25 Pa. The gas flow predictions, which do vary with basement pressure, were compared directly with tracer-entry measurements made at -30 Pa.

A sensitivity analysis was performed to determine the size of the error which might result from the changes in aspect ratio in adjacent elements due to the use of variable sized elements in the mesh. A close-up of the basement wall region was modeled with the flow-net terminating 7 m west of the wall and 4.3 m below the floor. The model was run twice, once with high resolution soil elements (167 elements total) allowing only small changes in size and

aspect ratio of adjacent elements and once with the wall and soil elements as they were in the main modeling effort (49 elements total). The deviation between the fine and coarse mesh predictions was less than five percent out to 2.5 m west of the house and less than ten percent beyond 2.5 m. Much of the deviation between the close-up models beyond 2.5 m is explained by boundary effects, as determined by comparing the results of the main modeling effort with those of the identical, close-up model. Therefore, the estimated uncertainty due to the use of variable-sized elements in the main modeling is probably less than five percent out to the D-row, and is certainly less than ten percent.

To quantify the effect of basement wall permeability on soil-gas entry, the permeability of the wall was varied among the cases modeled. Table I summarizes the permeabilities assigned to the wall elements in each of 10 cases. Results are presented for permeabilities ranging from 3×10^{-13} m^2 to 3×10^{-15} m^2. Because poured slab is estimated to be significantly less permeable than cement block, the cement-slab floor was assigned a low permeability of 3×10^{-20} m^2. This choice effectively limits entry to the wall area.

The permeable wall model applies to flow through uniform porous media (for example, homogeneous, porous building materials), to flow through a composite wall made up of different material types, or to flow through numerous small cracks in the cement block and/or mortar. In the latter two cases an effective permeability for the wall can be assigned as long as the channels through which flow occurs are small compared with the area over which flow is distributed. This is a common practice in hydrology when considering groundwater flow through a composite medium and in geology when considering fluid flow through cracks and fissures in rock. Therefore, in the current study *wall permeability* should be interpreted as an *effective permeability* of the wall.

Since the groundwater table at the site was known to be approximately 20 m below the surface, the soil was assumed to be unsaturated throughout the modeled region. Three configurations of the soil were modeled. In one case, the soil was specified as being uniform throughout, with a permeability of 3×10^{-12} m^2 (as indicated by in-situ measurements). The

second case tested the effect of a low-permeability soil layer just above basement floor level by assigning a permeability of 3 x 10^{-14} m^2 to the soil between 1.8 and 2.4-m depth, while the bulk of the soil was treated as in the first case. The permeability for this layer was based on the soil particle size analysis. The depth approximates that estimated in the field and was chosen for modeling convenience. The low-permeability soil layer was terminated 17 m to the west of the house because at greater distances the elements of the mesh were not fine enough to define such a thin layer. Termination of the layer at this distance will not result in distortion of the pressure field within 5 m of the house, the region for which we make a quantitative comparison with the data. The results will be less reliable for F-row probes, 14 m west of the house.

The third soil configuration tests the effect of incorporating a region with potentially distinct soil permeability next to the basement wall. Such a region can result from the process of backfilling the house excavation hole with soil after completion of basement construction. In the case of the field site, permeabilities measured in the backfill zone were similar to those in the bulk soil, but higher than those in the low-permeability layer. Therefore, for the backfill case, soil permeabilities were specified as for the layered-soil case except that the low-permeability layer was terminated 1.0 m from the house, the soil between 0.0 and 1.0 m being assigned the permeability of the bulk soil. The soil is assumed to be homogeneous and isotropic within each region.

Discussion of Modeling Results

Table II presents pressure-coupling predictions of the model (in percent of basement underpressure). A comparison of cases 1 through 3 demonstrates the effect of decreasing wall permeability on pressure-coupling in the soil. As expected, pressure-coupling decreases with decreasing wall permeability. In homogeneous soil, a reduction of wall permeability from 3 x 10^{-13} to 3 x 10^{-15} m^2 results in a reduction of predicted pressure-coupling from 50 to 6 percent in the A-row and from 18 to 2 percent in the D-row. A similar trend can be seen for

cases in which the soil is layered, and layered and backfilled (cases 4 and 5, and 6 and 7, respectively). The horizontal pressure gradient between rows A and D decreases with decreasing wall permeability as does the vertical pressure gradient between the soil surface and the A-row probe. By Darcy's Law, this reduced pressure gradient results in decreased soil-gas flow rates.

The addition of the low-permeability soil layer has little effect on near house pressure-coupling above the depth of the layer. Far-field coupling below the layer is, however, greatly increased in the presence of the layer (compare Figures 2 and 3). This phenomenon accounts for the high pressure-coupling observed at 3-m deep probes in the C, D, and E rows (Figure 1), whereas the homogeneous soil model does not (for example, Figure 2). The net effect of the low-permeability layer is to extend the zone of influence of the house in the deep soil. This effect, in combination with the leakage geometry of the house substructure, can be an important determinant of soil-contaminant entry rates. Especially since most sources would be expected, in the presence of a low-permeability soil layer, to have higher concentrations in deeper soil because of reduced dilution by surface air.

A comparison of cases 6, 7, and 10 with cases 4, 5, and 9, respectively (Table II), shows that the presence of the backfill region, as modeled, has little effect on predicted pressure-coupling. (The pressure contour map for the backfill case is almost identical to Figure 3.) For a given wall permeability, all soil configurations produce similar results in the near-field above the depth of the soil layer. This result would not be expected if the permeability of the backfill region was appreciably different from that of the bulk soil. For example, a very high permeability backfill zone should create a short circuit in the soil-gas flow path, reducing far-field coupling and flow.

A wall permeability of 9×10^{-14} m^2 gave a best fit to the measured average pressure-coupling (Tables I and II). This value is close to the permeability of 2×10^{-13} m^2 of cement block material coated with a mortar sealant estimated from the results of Maryowski's (16) tests of air-flow through cement block walls. Although Marynowski's measurements were made on

hollow block walls, a permeability can be calculated for the building material, subtracting out the effect of the void spaces by calculating an effective path length for air-flow through the solid medium.

The model was run using the "best fit" wall permeability for all soil configurations: namely, for unlayered soil, layered soil, and layered soil with a backfill (cases 8, 9, and 10, respectively). The pressures predicted for rows A through D at 1.5-m depth are presented in Table II. It is difficult to pick the best fit among the models from these data. However, as mentioned earlier, the high pressure-coupling measured in 3-m deep probes even out to 14 m from the house suggest that the soil is not homogeneous, whereas the layered-soil model gives a reasonable estimate of the observed coupling.

Also shown in Table II are predictions from the finite difference models of Mowris (13) and Loureiro (14) for the A through D row locations for one and ten millimeter wall-floor gap widths, for the case of homogeneous soil. Even for a gap as large as 10 mm, these models underpredict pressure-coupling at this site. Whereas, with a reasonable wall permeability of 9 x 10^{-14} m^2, the permeable wall model yields fairly accurate predictions. This result indicates that it is likely that entry occurred distributed over the wall area.

Figure 4 plots the soil-gas entry rate based on the current model for each of the ten cases considered. The output of the model is given in volumetric flow rate per unit of horizontal wall length (the third dimension--not included in the model) associated with each flux-boundary node. To estimate the rate of soil-gas flow into the basement, the sum of the wall fluxes are simply multiplied by the length of the wall adjoining the soil; the flux through the floor slab being negligible. The results indicate that soil-gas entry is slightly less than proportional to wall permeability. As the wall permeability decreases, the entry rate should converge on being proportional to the wall permeability, since the coupled resistance to flow presented by the soil and the wall will be dominated by the wall.

Since the model specifies that soil-gas entry occurs along the entire depth of the wall, but the majority of the wall is above the low-permeability soil layer, the presence or absence of

the layer has little effect on the entry rate (Figure 4). A quite different result would be expected if entry occurred primarily below the level of the soil layer (for example, if entry occurred through a gap at the wall-floor joint or through a permeable earthen floor). In that case, a low-permeability soil layer should obstruct the source of surface air, restricting soil-gas entry into the building.

The "best fit" wall permeability, determined by comparing the predicted with the measured pressure-coupling, also produced a reasonable prediction of the soil-gas entry rate. Using this permeability, both the layered and unlayered-soil models predicted entry rates of approximately 2.5 m^3hr^{-1} (last three cases, Figure 4), in reasonable agreement with the measured rate of 4 m^3hr^{-1}, with a range of 1.5 to 12 m^3hr^{-1}. By contrast a perimeter gap at the wall-floor interface cannot account for the measured entry, even assuming a large gap width. An analytical (closed form) model by Mowris and Fisk (1988) was used for calculating soil-gas entry into a house via a gap at the wall-floor interface. Using the geometric parameters of the study house, a basement depressurization of 30 Pa, and the average permeability of the bulk soil, the predicted soil-gas entry rate is 0.15 $m^3\ hr^{-1}$ for a 1-mm gap width, and 0.20 $m^3\ hr^{-1}$ for a 10-mm gap width, an order of magnitude below the measured value and the value predicted by the permeable wall model. This strongly suggests that, at the field site, entry occurred distributed over the wall area. This also suggests the importance that porous building materials might play in the entry of soil contaminants into houses. Even in houses which do have a wall-floor gap in the basement, transport through porous below-grade walls could dominate soil-gas entry.

Conclusions

This work demonstrates the potential importance of a previously neglected pathway for soil-gas entry into houses: pressure-driven flow through permeable, below-grade building materials. Such flow, distributed over the wall area, could occur through porous building materials or through a network of small cracks in subsurface walls and floors. If this pathway

is ignored, predictions of the rate of entry of soil gas into buildings could be substantially too low. For example, neglecting the permeable-wall pathway at the field site and assuming entry through a 10 mm gap at the wall-floor joint results in an order of magnitude underprediction of the soil-gas entry rate. Furthermore, in houses that do have a peripheral gap, entry through the gap could be small compared with entry through the walls.

A second factor, explored in a limited way, is the effect of a low-permeability soil layer just above basement floor level (such a layer was apparent at the field site). The layered-soil model predicts significantly higher far-field pressure-coupling below the layer than does the homogeneous soil model and helps to explain the high pressure-coupling observed at 3-m depth even out to 14 m from the house.

These findings have important implications for assessing human exposures to contaminants with a soil-gas source, such as radon and volatile organic contaminants. Wall permeability effects the rate at which soil gas may enter a house. Layering of the soil can determine the region from which soil gas is drawn and, therefore, the concentration of contaminants in the soil gas entering the building. Soil macrostructure also affects the shape of the pressure field, thereby determining the zone of influence of the house and the strength of pressure-coupling in different regions. These factors are crucial for understanding and predicting concentrations of contaminants in indoor air.

The results of this study also have bearing on indoor air pollution mitigation techniques. Entry through walls could explain why the sealing of gaps and penetrations in building substructures has been found to be relatively ineffective as a radon-entry mitigation measure (9). For houses in which entry via permeable walls is important, impermeable wall coatings might be a useful mitigation technique, reducing the need for expensive alternatives such as basement overpressurization, sub-slab depressurization, and crawl-space ventilation.

More research is needed in order to determine the magnitude and frequency of soil-gas entry through permeable building materials in the existing housing stock. More data are needed on the permeability of various building materials and sealants. In particular, tests

should be made on constructed walls, such as cement-block walls sealed and backfilled with cement. With data such as these, and with information on current building design, modeling could be used more effectively to assess the magnitude of soil-gas entry in the existing housing stock. These studies could, in turn, be used to ensure that future building practices minimize indoor air pollution by limiting soil-gas entry.

Acknowledgments

The authors would like to thank Nicholas Sitar for providing the finite element model. We are grateful for the editorial comments of Al Hodgson, Joan Daisey, William Nazaroff, William Fisk, and Nicholas Sitar.

Literature Cited

(1) Nero, A.V.; Nazaroff, W.W. *Radiat. Prot. Dosim.* **1984**, 7, 23-39.

(2) DSMA Atcon Ltd. *Review of Existing Information and Evaluation for Possibilities of Research and Development of Instrumentation to Determine Future Levels of Radon at a Proposed Building Site*; Atomic Energy Control Board: Ottawa, 1983; INFO-0096.

(3) Sextro, R.G.; Moed, B.A.; Nazaroff, W.W.; Revzan, K.L.; Nero, A.V. In *Radon and Its Decay Products: Occurrences, Properties, and Health Effects*; Hopke, P., Ed.; American Chemical Society: Washington D.C., 1987; Chapter 2.

(4) Nazaroff, W.W.; Moed, B.A.; Sextro, R.G. In *Radon and Its Decay Products Indoors*; Nazaroff, W.W.; Nero, A.V., Eds.; Wiley: New York, 1988; Chapter 2.

(5) Wood, J.A.; Porter, M.L. *J. Air Pollution Control Assoc.* **1987**, 37, 609-615.

(6) Hodgson, A.T.; Garbesi, K.; Sextro, R.G.; Daisey, J.M. *J. Air Pollution Control Assoc.*, in press.

(7) Turk, B.H.; Prill, R.J.; Fisk, W.J.; Grimsrud, D.T.; Moed, B.A.; Sextro, R.G. *Radon and*

Remedial Action in Spokane River Valley Homes, Volume 1; Lawrence Berkeley Laboratory: Berkeley, CA, 1987; LBL-23430.

(8) Turk, B.H.; Prill, R.J.; Sextro, R.G.; Harrison, J. In *Proceedings of the 1988 Symposium on Radon and Radon Reduction Technology*; Denver, CO; U.S. Environmental Protection Agency: Denver, CO, 1988; Paper. No. VI-3.

(9) Turk, B.H.; Prill, R.J.; Fisk, W.J.; Grimsrud, D.T.; Moed, B.A.; Sextro, R.G. In *Proceedings of the 79th Annual Meeting of the Air Pollution Control Association*; Minneapolis, MN; Air Pollution Control Association: Pittsburgh, PA, 1986; Paper No. 86-43.2.

(10) Nazaroff, W.W.; Lewis, S.R.; Doyle, S.M.; Moed, B.A.; Nero, A.V. *Environ. Sci. Technol.* **1987**, 21, 459-466.

(11) Nazaroff, W.W.; Doyle, S.M. *Health Physics* **1985**, 48, 265-281.

(12) Nazaroff, W.W.; Feustel, H.; Nero, A.V.; Revzan, K.L.; Grimsrud, D.T.; Essling M.A.; Toohey, R.E. *Atmos. Environ.* **1985**, 19, 31-46.

(13) Mowris, R.J. *Analytical and Numerical Models for Estimating the Effect of Exhaust Ventilation on Radon Entry in Houses with Basements or Crawl Spaces*; Lawrence Berkeley Laboratory: Berkeley, CA, 1986; LBL-22067.

(14) Loureiro, C.O. *Simulation of the Steady-state Transport of Radon from Soil into Houses with Basements Under Constant Negative Pressure*; Lawrence Berkeley Laboratory: Berkeley, CA, 1987; LBL-24378.

(15) Mowris, R.J.; Fisk, W.J. *Health Physics*, **1988**, 54, 491-501.

(16) Marynowski, J.M. *Measurement and Reduction Methods of Cinder Block Wall Permeabilities*; Center for Energy and Environmental Studies: Princeton University, Princeton,

NJ 1988; Working Paper No. 99.

(17) Harris, B.B, Ruppersberger, J.S.; Walton, M. Presented at *1988 Symposium on Radon and Radon Reduction Technology*; Denver, CO; U.S. Environmental Protection Agency: Denver, CO, October 1988.

(18) Hillel, D. *Fundamentals of Soil Physics*; Academic Press: New York, 1980, Chapter 11.

(19) Conner, J.J.; Brebbia, C.A. *Finite Element Techniques for Fluid Flow*; Newnes-Butterworths: Boston, 1976.

This work was supported by the Occidental Chemical Corporation under Agreement No. BG 8602A and by the Assistant Secretary for Conservation and Renewable Energy, Office of Building and Community Systems, Building Systems Division of the U.S. Department of Energy under Contract No. DE-AC03-76SF00098.

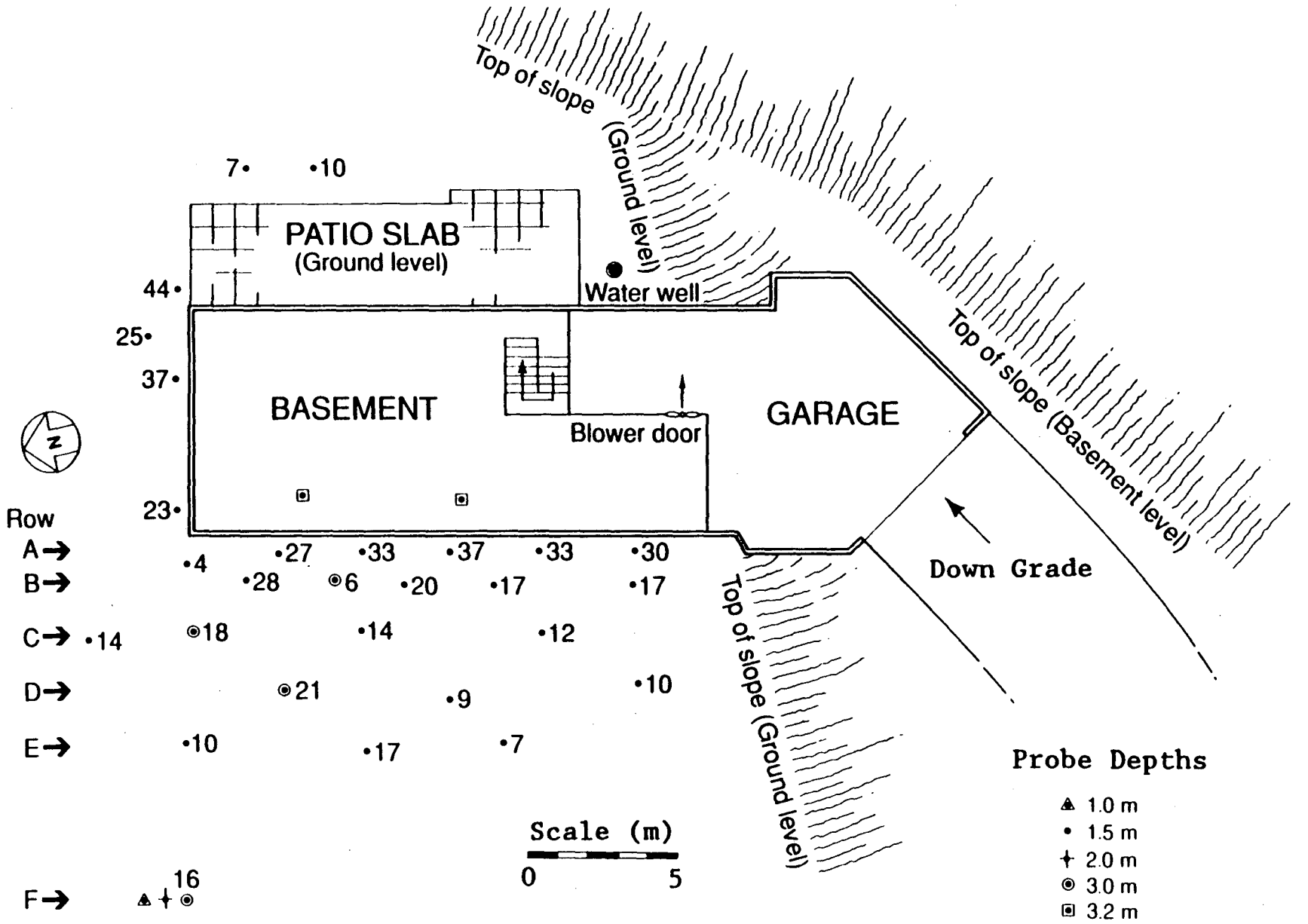

Figure 1. Plan view of the field site showing the basement-level floor plan and soil probe locations. Pressures measured at the probes are given in percent of basement depressurization. All probe depths are relative to ground level.

XCG 883-6553

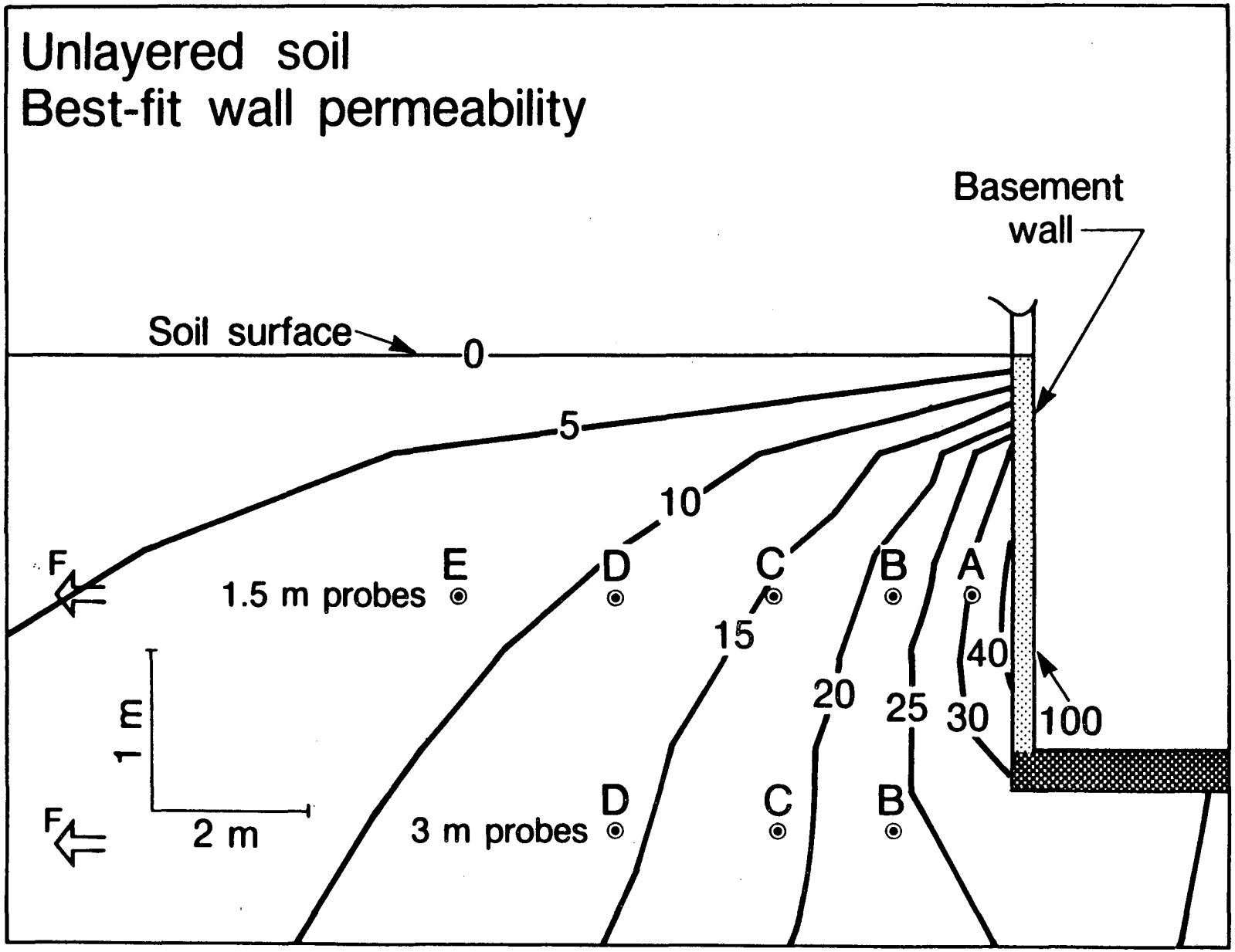

XBL 893-7066

Figure 2. Pressure contour map generated by the finite element model for the case of unlayered soil and 'best fit' wall permeability (case 8, Ubn). Pressure contours are given in percent of basement underpressure. Soil probe locations are marked by bull's-eyes.

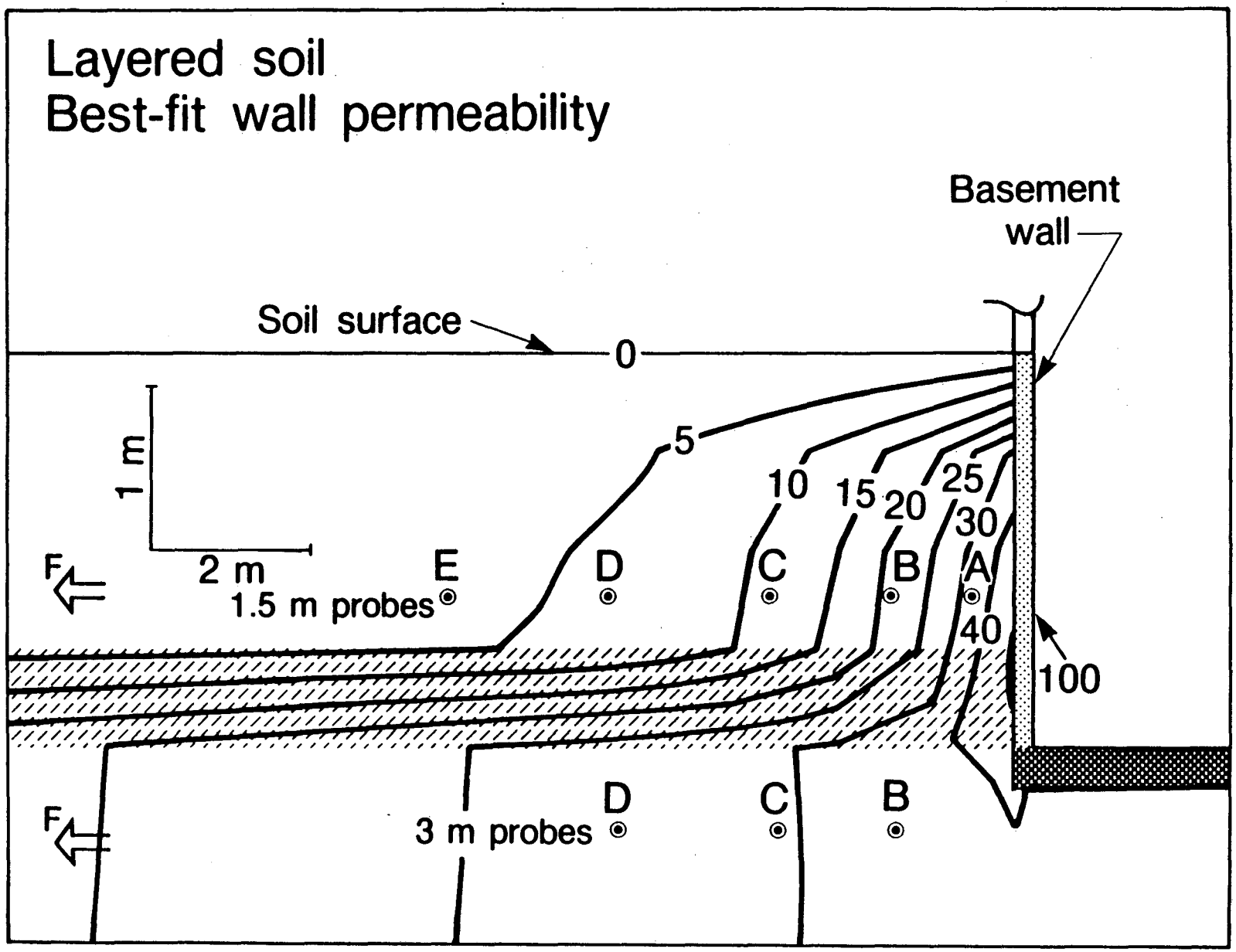

Figure 3. Pressure contour map generated by the finite element model for the case of layered soil and 'best fit' wall permeability (case 9, Lbn). The shaded area indicates the low-permeability soil layer. Pressure contours are given in percent of basement underpressure. Soil probe locations are marked by bull's-eyes.

XBL 893-7067

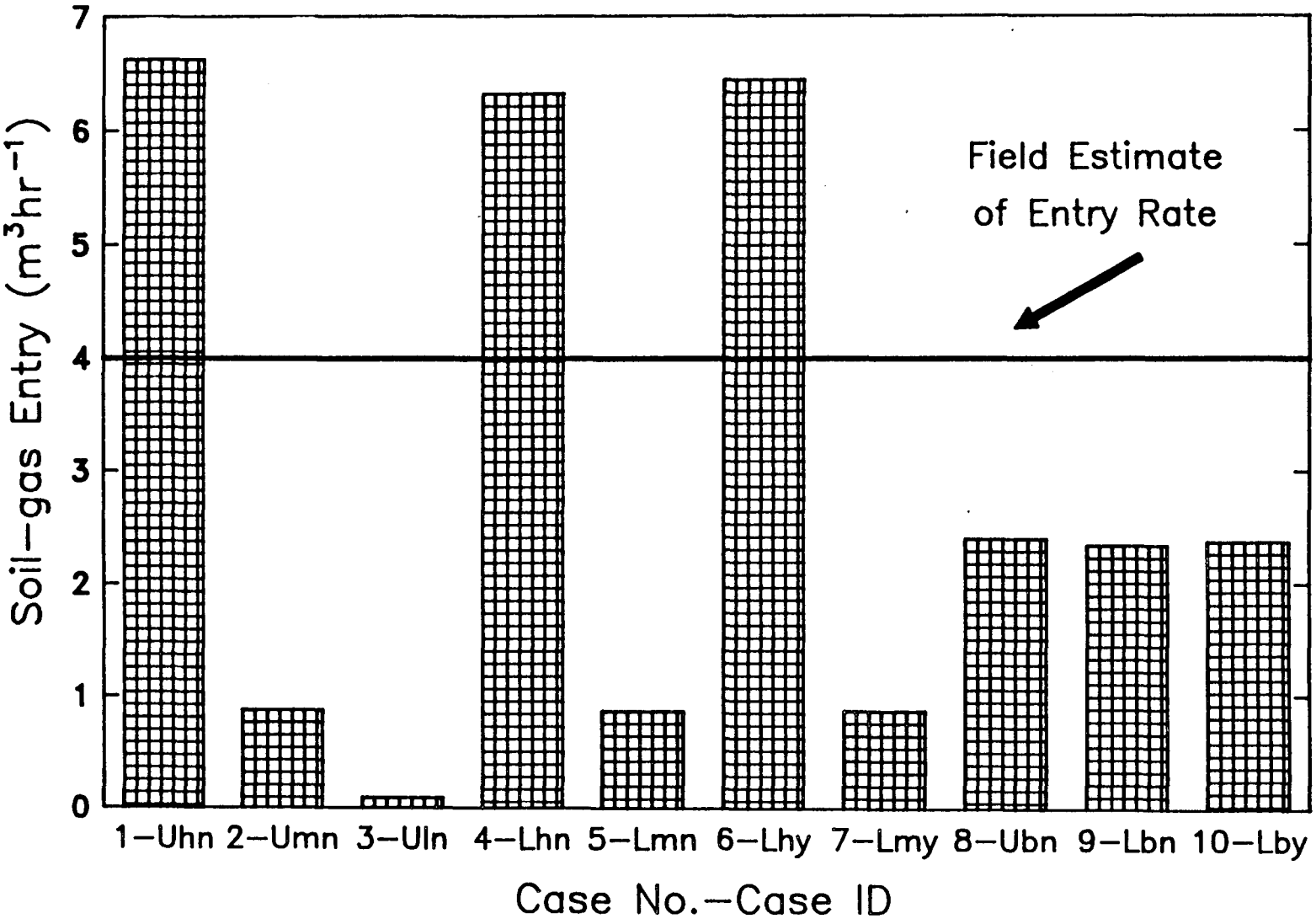

Figure 4. Entry rate of soil gas into the basement predicted by the finite element model for a basement pressure of -30 Pa. The bold line at 4 m^3hr^{-1} shows the best estimate for soil-gas entry based on experimental data. (See Table I for explanation of case number and ID.)

Table I. Descriptions of each case of the finite element model specifying case ID and wall permeability.

Case No.	Case Description			Case ID[d]	Wall Permeability (m^2)
	soil[a]	wall[b]	backfill[c]		
1	unlayered	high	no	Uhn	3×10^{-13}
2	unlayered	medium	no	Umn	3×10^{-14}
3	unlayered	low	no	Uln	3×10^{-15}
4	layered	high	no	Lhn	3×10^{-13}
5	layered	medium	no	Lmn	3×10^{-14}
6	layered	high	yes	Lhy	3×10^{-13}
7	layered	medium	yes	Lmy	3×10^{-14}
8	unlayered	best fit	no	Ubn	9×10^{-14}
9	layered	best fit	no	Lbn	9×10^{-14}
10	layered	best fit	yes	Lby	9×10^{-14}

a. Soil configuration: unlayered or layered.

b. Wall permeability: high, medium, low, or "best fit."

c. Backfill: yes, if present; no, if absent.

d. Case ID designated by the first letter of the soil, wall, and backfill descriptions.

Table II. Pressure coupling at 1.5 m depth predicted by the permeable wall model used here and by perimeter gap models of other authors, and averaged pressure-coupling determined by field measurements. All table values are percentages of basement depressurization. The table is divided into four sections designated 'range', 'best fit', 'data', an 'other models'. 'Range' represents cases which present the range of wall permeabilities, corresponding to the first seven cases of Table I. 'Best fit' correspond to the last three cases in Table I, where the wall permeability is picked to produce a best fit to the field data, 'data'. 'Other models' gives the pressure coupling predicted by the numerical models of Mowris (1986) and Loureiro (1987) for a basement wall-floor gap width of 1 and 10 mm.

	Case No.	Case ID	Ring designation (distance from house (m)) A(0.5)	B(1.5)	C(3.0)	D(5.0)
RANGE						
	1	Uhn	50	36	25	18
	2	Umn	19	13	9	7
	3	Uln	6	4	3	2
	4	Lhn	51	34	18	10
	5	Lmn	20	13	7	4
	6	Lhy	52	36	19	10
	7	Lmy	22	14	7	4
BEST FIT						
	8	Ubn	31	22	15	11
	9	Lbn	32	21	12	6
	10	Lby	33	23	12	6
DATA[a]			32	21	13	10
OTHER MODELS						
		Mowris (1 mm)	11	8	5	3
		Mowris (10 mm)	11	10	6	4
		Loureiro (1 mm)	8	6	4	2
		Loureiro (10 mm)	12	8	6	3

a. Data values are the average value for 1.5-m deep, west-side probes in each row. One data point on the NW corner of the house with 4% coupling was omitted from the data-set as an obvious outlyer (see Figure 1).

LAWRENCE BERKELEY LABORATORY
TECHNICAL INFORMATION DEPARTMENT
1 CYCLOTRON ROAD
BERKELEY, CALIFORNIA 94720